Current Applied Physics 11 (2011) S376–S380

Contents lists available at ScienceDirect

Current Applied Physics

journal homepage: www.elsevier.com/locate/cap

Electro-conducting polymeric films prepared from the hybrids of carbon nanotubes and graphene nanosheets

Do Hyeong Kim, Young Soo Yun, Hyeonseong Bak, Se Youn Cho, Hyoung-Joon Jin*

Department of Polymer Science and Engineering, Inha University, Incheon 402-751, Republic of Korea

ARTICLE INFO

Article history:
Received 3 December 2010
Received in revised form
26 February 2011
Accepted 14 March 2011
Available online 21 March 2011

Keywords:
Graphene
Transparent conducting film
Single-walled carbon nanotubes

ABSTRACT

Transparent and electro-conducting hybrid films were fabricated from unoxidized graphene nanosheets and single-walled carbon nanotubes (SWCNTs). A graphene dispersion was prepared in N-methylpyrrolidone (NMP) with ultrasonication. This ultrasonication method allows the preparation of unoxidized graphene nanosheets. Therefore, graphene nanosheets could be obtained with a low defect concentration and good electro-conductivity. In the hybrid films of graphene nanosheets and SWCNTs, the graphene nanosheets were interconnected by SWCNTs. A transparent hybrid film with relatively low sheet resistance could be prepared because this interconnected structure between the SWCNTs and graphene nanosheets can act as an electro-conducting pathway. As a result, the hybrid film showed improved electrical, transparent characteristics using unoxidized graphene, even though a small amount of SWCNTs were used. The hybrid films had 90% transmittance at 550 nm and a sheet resistance of 1.9×10^3 Ω/sq.

1. Introduction

Considerable effort has been made toward the synthesis of transparent conducting (TC) films because of their use in device technologies, such as touch screens, organic light emitting diodes, flat panel displays [1–8]. Indium tin oxide (ITO) is used most commonly in TC films but it has the following disadvantages [1,2,4,5,9]: (1) ITO is inherently inefficient with plastic substrates because of its high temperature processing, (2) the cost of the materials has increased sharply, and (3) ITO cannot be applied to flexible TC films because of its brittle nature. Therefore, alternative, mechanically flexible and more cost-effective materials are needed to replace ITO.

Single-walled carbon nanotubes (SWCNTs) are considered one of the most promising candidates for TC films [1–3] owing to their outstanding electrical and mechanical (flexibility) properties and high thermal stability. In recent studies, SWCNTs were used to prepare TC films. These films exhibited 80–85% of transmittance and a sheet resistance of 200–500 Ω/sq [1]. Therefore, these films are suitable as transparent conductors. On the other hand, a TC film using SWCNTs has a limitation in terms of transparency despite its high electro-conductivity.

Graphene is a single atomic layer of carbon, which has been studied for its potential in TC devices [8,10]. Graphene has a large surface area, (theoretical value of 2600 m^2/g) [11] remarkable mechanical stiffness and excellent electrical conductivity.

In particular, graphene, which is an atomically thick layer of graphite, is extremely thin and has remarkable transmittance. Furthermore, the low cost of graphite, which is a precursor for graphene, makes graphene a promising candidate for TC films [11,14–16].

Graphene nanosheets can be fabricated from graphite by chemical exfoliation and reduction methods [4,5] or mechanical exfoliation methods [9,11]. Chemical exfoliation and reduction methods involve the chemical oxidation of graphite to hydrophilic graphite oxide, which can be readily exfoliated as individual graphene oxide (GO) nanosheets through ultrasonication in water. GO, which is electrically insulating, can be converted back to conducting graphene through a chemical reduction but this process results in a significant number of defects that continue to disrupt the electrical properties [12]. The mechanical exfoliation method consists of the direct exfoliation of graphite using sonication in specific organic solvents, such as N-methylpyrrolidone and benzyl benzoate [13]. This method can produce high-quality, unoxidized graphene nanosheets.

Some techniques have been devised to prepare CNT–GO hybrid films. Tung et al. reported a method that a CNT–GO mixture solution was deposited onto a PET substrate through spin-coating with spray coating [6]. This method has been used to deposit uniform thin films onto PET substrates. In addition, Wang et al. reported a transfer printing method [5], where a GO mixing solution was vacuum-filtered through a membrane, and the membrane was then pressed onto a quartz substrate to transfer the GO layer. However, hydrazine, a highly toxic material, was used to reduce GO to graphene in both methods.

* Corresponding author. Fax: +82 32 865 5178.
E-mail address: hjjin@inha.ac.kr (H.-J. Jin).

1567-1739/$ – see front matter © 2011 Elsevier B.V. All rights reserved.
doi:10.1016/j.cap.2011.03.052

In the present study, TC films were fabricated using unfunctionalized SWCNTs dispersions in N-methylpyrrolidone (NMP) and unoxidized graphene dispersions that were prepared by physical exfoliation in NMP. Vacuum filtration was used to produce hybrid SWCNT–Graphene films. The films exhibited a low sheet resistance with very small amounts of graphene nanosheets because the SWCNTs acted as an electrical bridge for the network. The sheet resistance of the film could be improved by increasing the amount of SWCNTs in the TC film composed of only SWCNTs. On the other hand, the transmittance of the film would be decreased in such a case. The transmittance of SWCNT–Graphene hybrid films was increased considerably and the sheet resistance was decreased compared to the TC film composed of only SWCNTs. This results from the use of a two-dimensional graphene nanosheet with high transmittance and high electro-conducting characteristics.

2. Experiment

2.1. Materials

The graphite powder was purchased from Sigma–Aldrich (Product Number 332461). NMP was obtained from Sigma–Aldrich. The SWCNTs were supplied by the Hwanwha Nanotech Co., Korea. The SWCNTs were synthesized using the arc discharge method, and a PET film (skyrol® SH40) from SK corporation was used to fabricate the transparent conducting films.

2.2. Preparation of SWNT-Graphene dispersions in NMP

Graphite was dispersed in the NMP solvent (cylindrical vial, 50 ml solvent) at a concentration of 1 mg/ml by ultrasonication in a bath type ultrasonicator for 30 min. The dispersion was centrifuged using a Jouan MR 23i centrifuge for 90 min at 500 rpm. After centrifugation, the sample was decanted by pipetting off the top half of the dispersion. The SWCNTs were dispersed in NMP solvent at 1 mg/ml by sonication for 90 min.

2.3. Preparation of electrically conductive and transparent films

The SWCNT–Graphene was deposited onto Anopore Inorganic Membranes (pore size: 20 nm) through vacuum filtration. Subsequently, it was dried overnight in a vacuum oven at 80 °C. The SWCNT–Graphene hybrid face was sandwiched between the PET film and membrane surface. When a pressing force of 0.25 ton at 200 °C was applied, the SWCNT–Graphene was transferred to PET substrate due to the better interaction between the SWCNT–Graphene and PET film.

2.4. Characterization

After the samples were pre-coated with a homogeneous Pt layer by ion sputtering (E-1030, Hitachi, Japan), field-emission scanning electron microscopy (FE-SEM, S-4300SE, Hitachi, Japan) was carried out at an accelerating voltage of 15 kV to observe the surface morphology of the hybrid films. Field-emission transmission electron microscopy (TEM, CM200, Philips, Netherlands) was used to confirm the presence of graphene nanosheets in the NMP solvent, and the samples were prepared by drop casting of the dispersion onto holey carbon grids. The thickness of the graphene nanosheets was observed by atomic-force microscopy (AFM, SPA400, Seiko Ins., Japan) operated in tapping mode. Turbiscan analysis exhibited dispersion stabilities of SWCNT and graphene dispersions. FT-Raman (RFS 100/S/bruker) analysis was used to characterize the chemical structures of the graphene nanosheet on a PET film. The

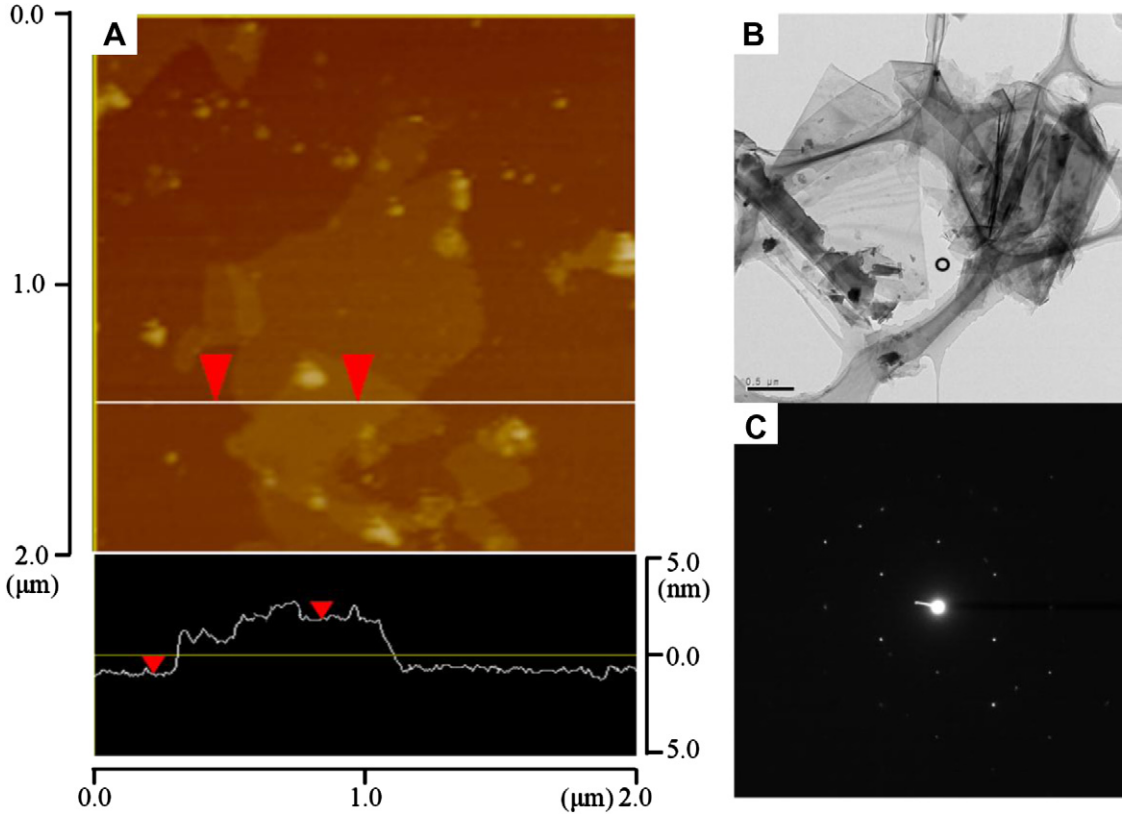

Fig. 1. Characterization of the graphene nanosheets. (A) Typical tapping-mode AFM image of graphene nanosheets deposited on a silica substrate. High-resolution TEM image (B) of the graphene nanosheets (scale bar 1 μm) and (C) the select area electron diffraction pattern taken from the position of the dark round spot in the TEM image.

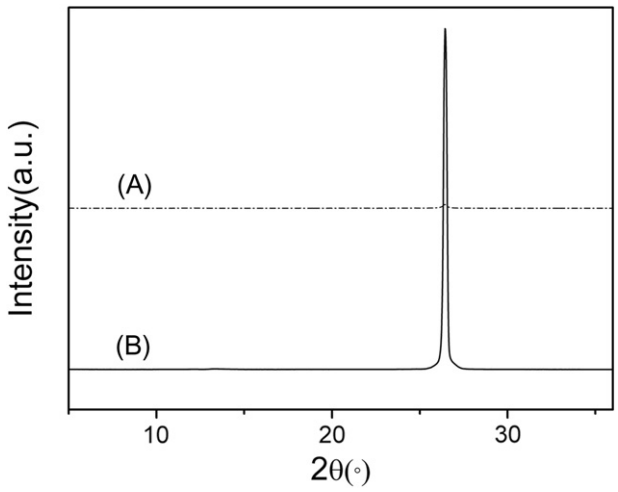

Fig. 2. X-ray diffraction patterns of (A) graphene after ultrasonication in an NMP solvent and (B) pristine graphite.

chemical structures of graphene and graphite were examined by X-ray diffraction (XRD, RigakuDMAX2500) using CuKα radiation (wavelength $\lambda = 0.154$ nm). An Agilent 8453 UV–visible spectrophotometer (Agilent Technologies, Germany) was used to measure the transmittance of the electrically conducting transparent films over the wavelength range, 380–750 nm. A four-probe method with an electrical conductivity meter (Loresta GP, Mitsubishi Chemical, Japan) was used to measure the electrical conductivity of the hybrid films and SWCNT films.

3. Results and discussion

In many groups, SWCNTs have been exfoliated successfully using N-methylpyrrolidone (NMP). Using the same system, graphene also exhibited similar behavior. Fig. 1-A shows a typical tapping-mode atomic-force microscopy (AFM) image of a few graphene nanosheets deposited onto a silica substrate. An analysis of the AFM image revealed graphene nanosheets with heights of approximately 1.59–3 nm, which indicates 3–6 graphene nanosheet layers. In Fig. 1-B, the TEM image showed that the graphite

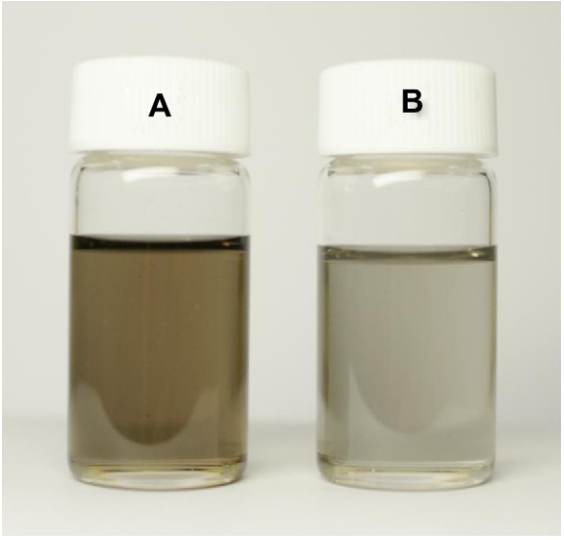

Fig. 3. Optical images of the dispersion statements. (A) Dispersion of the SWCNT in NMP and (B) dispersion of graphene in NMP.

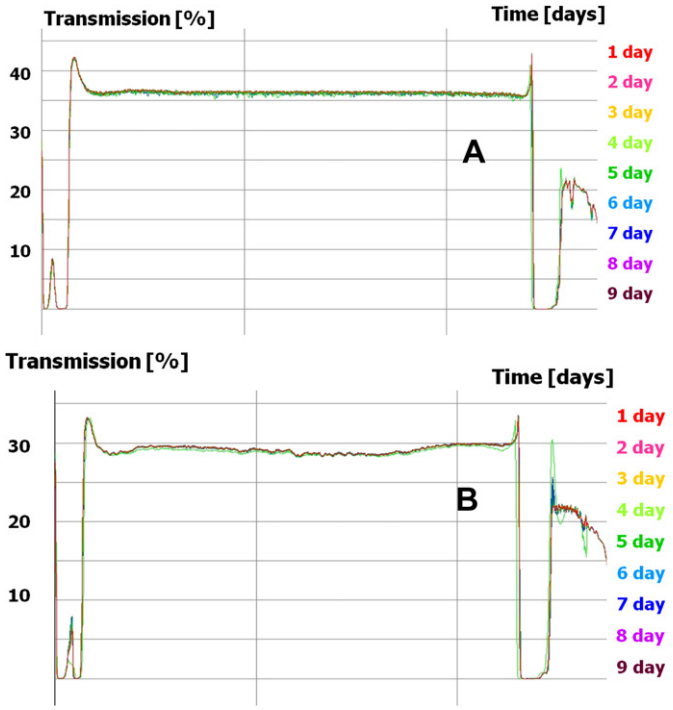

Fig. 4. Turbiscan data of (A) the graphene dispersion (0.001 mg/mL) in pure NMP and (B) the SWCNT dispersion (0.001 mg/mL) in pure NMP.

was exfoliated in the NMP by ultrasonication [13]. The graphene nanosheets were exfoliated according to the bright-field TEM image. TEM and AFM revealed the size of the graphene nanosheets (1–2 μm). Select area electron diffraction (SAED) of the graphene nanosheets (Fig. 1-C) exhibited a hexagonal pattern, corresponding to reflected monolayer graphene [13].

Fig. 2 shows the XRD patterns of pristine graphite and graphene. A strong and sharp diffraction peak at 26.6° was observed for the pristine graphite because of the stacked graphite that was aligned along the (002) plane. Nevertheless, no apparent diffraction peaks were detected for the graphene that had been exfoliated through ultrasonication, confirming that the graphene nanosheets had been exfoliated quite well [14].

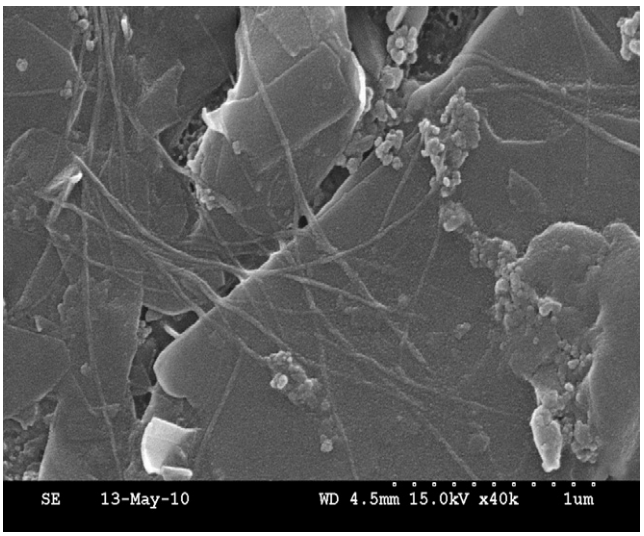

Fig. 5. FE-SEM images of the SWCNT (0.002 mg)–graphene(0.01 mg) hybrid dispersion on the pure PET films using the vacuum filtration method.

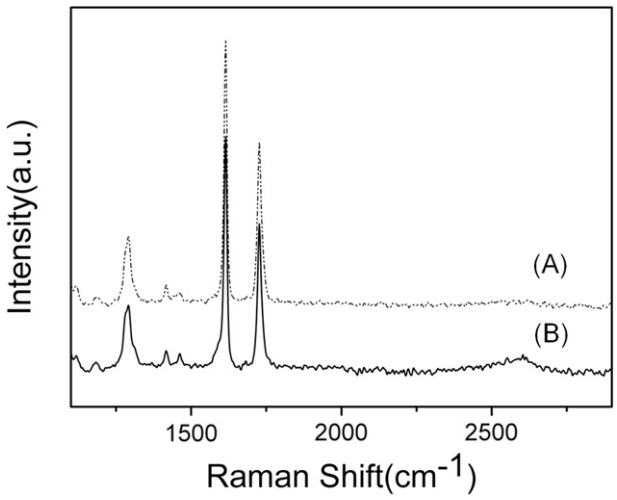

Fig. 6. Raman spectra of (A) pure PET film and (B) the graphene nanosheets that were deposited on the PET film by vacuum filtration.

The formation of the stable graphene and SWCNT dispersions in NMP was observed using the turbiscan spectra and optical image. The optical image (Fig. 3) showed that the graphene and SWCNT dispersions were well dispersed in the NMP solvent after 1 week. The turbiscan spectra showed that the graphene (Fig. 4A) and SWCNT (Fig. 4B) dispersions were stable in NMP.

The morphology and microstructure of the SWCNT–graphene hybrid TC films were characterized by SEM (Fig. 5). The SWCNT and graphene nanosheet were well mixed. The graphene nanosheets were interconnected by SWCNTs because of their 1D morphology with a high aspect ratio. This interconnected structure between the SWCNTs and graphene nanosheets can act as an electro-conducting pathway [6]. In the present study, by reason of their morphological characteristics, which are a 1D or 2D structure with a high aspect ratio, the SWCNT–graphene hybrid TC film easily forms an electrical network at low SWCNTs concentrations compared to the TC film with only SWCNTs.

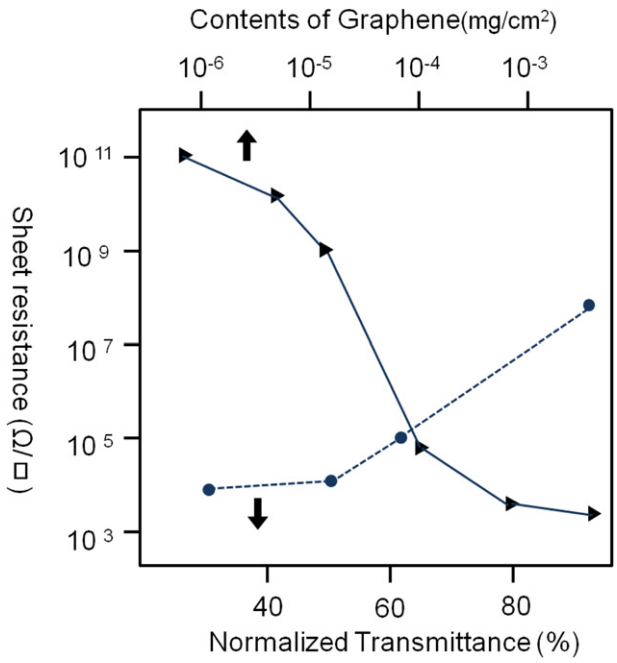

Fig. 7. Normalized transmittance and contents of graphene nanosheets as a function of the sheet resistance of the graphene films.

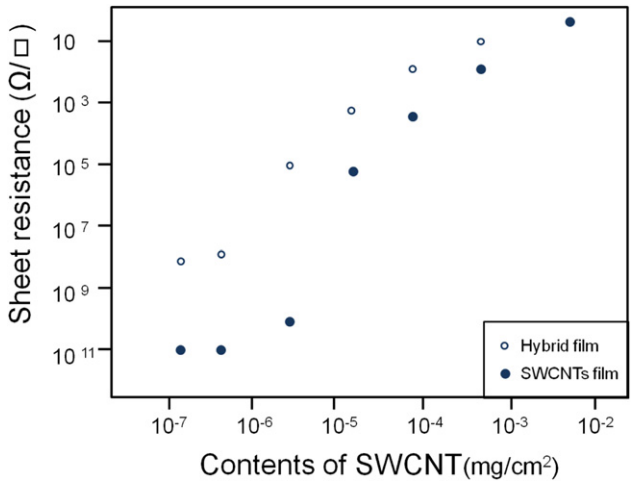

Fig. 8. Sheet resistance of the SWCNT–graphene hybrid films and SWCNT films as a function of the SWCNT contents.

Fig. 6 shows the Raman spectra of (A) the PET film spectrum and (B) graphene nanosheets on the PET film. The G-band ($\sim$1580 cm^{-1}), D-band ($\sim$1350 cm^{-1}), and 2D-band (2600 cm^{-1}) were clearly visible in both cases. The G-band indicated the graphite carbon structure (sp^2). The D-band showed the typical defects in the carbon material. The 2D-band confirmed the quality of exfoliation. Nevertheless, the difference in the G-band and D-band peaks between graphene on PET and the raw PET film could not be determined because the PET peaks were too strong, and the graphene peaks did not appear. The existence of graphene was confirmed using the 2D-band, which was stronger than the raw PET films [15–17].

Fig. 7 shows the transmittance and contents of graphene as a function of the sheet resistance of the only graphene transparent conductivity films. The obtained graphene nanosheets on the PET substrates showed sheet resistances of 3.2×10^8, 1.9×10^5, 3.8×10^4 and 3.2×10^4 Ω/sq for transparencies (defined as the transmittance at 550 nm) of 93.3%, 67%, 51% and 30% respectively. The sheet resistance increased gradually with increasing transmittance. At a graphene content of 7.96×10^{-4} mg/cm^2 or above, the graphene films exhibited the percolation threshold of the sheet resistance. For graphene contents $<10^{-3}$ mg/cm^2, the optical transmittance

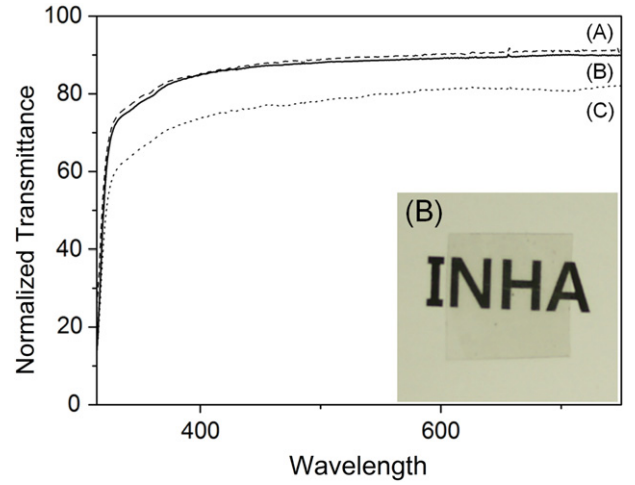

Fig. 9. UV–vis spectra of (A) SWCNT–graphene hybrid film on pure PET films, and (B) SWCNT film on the pure PET films (Inner: Optical photographs of (A) the hybrid film).

was generally >82%, whereas the sheet resistance varied from 10 MΩ/sq to 100 MΩ/sq.

Fig. 8 shows the sheet resistance of the SWCNT films and hybrid films. At low levels of SWCNTs in the films, the sheet resistance did not change according to the SWCNT contents. On the other hand, with SWCNT contents $>1.59 \times 10^{-4}$ mg/cm^2, the SWCNT films exhibited the percolation threshold of the sheet resistance because the SWCNTs formed an electrical network. In the case of hybrid films, they showed better sheet resistance than the SWCNT films because the hybrid films already included 7.96×10^{-4} mg/cm^2 graphene. We suggest the formation of an extended conjugated network with individual SWCNTs bridging the gaps between graphene sheets. The two-dimensional large graphene sheets cover the majority of the total surface area, whereas the SWCNTs act as wires connecting the large pads together. Therefore, the hybrid films exhibited an electrical percolation threshold at low amounts of SWCNTs compared to the only SWCNTs films.

Fig. 9 indicates the normalized UV–vis spectra of the graphene-only films (A), SWCNT–graphene hybrid films (B) and the SWCNT films (C). A bare PET substrate was used as the background. The graphene films showed an optical transmittance of 92% and a low quality sheet resistance of only 2.2×10^7 Ω/sq. This sheet resistance was induced by so much free volume indicating that the number of inter graphene nanosheet junctions was much lower than that expected for a dense film. Therefore, the SWCNT bridged the gap between the graphene nanosheets to improve the sheet resistance.

The UV–vis spectra of hybrid films and SWCNT film reveal the transmittance of these films with a sheet resistance of 1.9×10^3 Ω/sq on a PET substrate. The hybrid film showed higher optical transmittance (90% at 550 nm) than the SWCNT film (80% at 550 nm) and the sheet resistance of the hybrid film was decreased by the addition of SWCNTs [18]. The hybrid film prepared with 7.96×10^{-4} mg/cm^2 graphene and 1.59×10^{-4} mg/cm^2 SWCNT had a mean sheet resistance of 1.9×10^3 Ω/sq, which was better than the only SWCNT film with the same transmittance (90%).

4. Conclusions

TC hybrid films were prepared from graphene nanosheets and SWCNTs. Graphene nanosheets with low defect concentrations were prepared using a mechanical exfoliation method with ultrasonication. In the hybrid films, the graphene nanosheets were interconnected by SWCNTs owing to their 1D morphology and high aspect ratio. Therefore, the SWCNT–graphene hybrid film easily formed an electrical network at low SWCNT contents compared to the TC film with only SWCNTs. The TC hybrid films had a sheet resistance of 1.9×10^3 Ω/sq and a transmittance of 90%. These results surpassed the performance of the SWCNT films, which have a similar sheet resistance.

Acknowledgment

This work was supported by the grant from the Industrial technology development program of the Ministry of Knowledge Economy (MKE) of Korea.

References

[1] I.S. Young, C.M. Yang, D.Y. kim, H. Kanoh, K. Kaneko, J. Colloid Interface Sci. 318 (2008) 365–371.
[2] L.H. Sondra, H.W. Lee, Zhenan Bao, ACS Nano 3 (2009) 1423–1430.
[3] Zhu. Wu, Zhi. Chen, Xu Du, J.M. Logan, J. Sippel, M. Niko, K. Kamaras, J.R. Reynolds, D.B. Tanner, A.F. Hebard, A.G. Rinzler, Science 305 (2004) 1273–1276.
[4] J. Wu, M. Agrawal, H.A. Becerril, Z. Bao, Z. Liu, Y. Chen, P. Peter, ACS Nano 4 (1) (2010) 43–48.
[5] S.J. Wang, Y. Gang, Q. Zheng, J.K. Kim, Carbon 48 (2010) 1815–1823.
[6] V.C. Tung, L.M. Chen, M.J. Allen, J.K. Wassei, K. Nelson, R.B. Kaner, Yang Yang, Nano Lett. 9 (5) (2009) 1945–1955.
[7] Rong kou, Y. Shao, D. Wang, M.H. Engelhard, J.H. Kwak, J. Wang, V.V. Viswanathan, C. Wang, Y. Lin, Y. Wang, I.A. Aksay, Jun. Liu, Electrochem. Commun. 11 (2009) 954–957.
[8] T. Ihn, J. Gűttinger, F. Molitor, S. Schnez, E. Schurtenberger, A. Jacobsen, S. Hellműller, T. Frey, S. Drőscher, C. Stampfer, K. Ensslin, Mater. Today 3 (3) (2010) 44–50.
[9] K. Jonathan, Richard Wassei, B. Kaner, Mater. Today 3 (3) (2010) 52–59.
[10] Y. Lee, S. Bae, H. Jang, S. Jang, S.E. Zhu, S.H. Sim, Y.I. Song, B.H. Hong, J.H. Ahn, Nano Lett. 10 (2010) 490–493.
[11] J.M. Kim, F. Kim, J. Huang, Mater. Today 13 (2010) 28–38.
[12] D. Li, M.B. Műller, S. Gilje, R.B. Kaner, G.G. Wallace, Nat. Tech. 3 (2008) 101–105.
[13] Y. Hernandez, V. Nicolosi, M. Lotya, F.M. Blighe, Z. Sun, S. De, I.T. Mcgovern, B. Holland, M. Byrne, Y.K. Gunko, J.J. Boland, P. Niraj, G. Duesberg, S. Krishnamurthy, R. Goodhue, J. Huthe, T. Chison, V. Scardaci, A.C. Ferrari, J.N. Coleman, Nat. Nano 3 (2008) 563–568.
[14] H.B. Zhang, W.G. Zheng, Q. Yan, Y. Yang, J.W. Wang, Z.H. Lu, G.Y. Ji, Z.Z. Yu, Polymer 51 (2010) 1191–1196.
[15] Y. Liang, D. Wu, X. Feng, K. Műllen, Adv. Mater. 21 (2009) 1679–1683.
[16] I. Calizo, A.A. Balandin, W. Bao, F. Miao, C.N. Lau, Nano Lett. 7 (2007) 2645–2649.
[17] J. Štokr, B. Schenider, D. Doskočilova, J. Lővy, Polymer 23 (1982) 714–721.
[18] R.J. Narayan, S.P. Adiga, M.J. Pellin, L.A. Curtiss, S. Stafslien, B. Chisholm, N.A. Monteiro, R.L. Brigmon, J.W. Elam, Mater. Today 13 (2010) 60–64.